

NON-BASELINE DETECTION OF SMALL DAMAGES FROM CHANGES IN STRAIN ENERGY MODE SHAPES

EDWARD S. SAZONOV^{a,*}, POWSIRI KLINKHACHORN^a, UDAYA B. HALABE^b and
HOTA V.S. GANGARAO^b

^a*Lane Department of Computer Science and Electrical Engineering, P.O. Box 6109, College of
Engineering and Mineral Resources, West Virginia University, Morgantown, WV 26506, USA;*

^b*Department of Civil and Environmental Engineering, Constructed Facilities Center, West Virginia
University, Morgantown, WV 26506, USA*

(Received 11 February 2002; In final form 10 May 2002)

Several methods for damage detection based on identifying changes in strain energy mode shapes (SEMS) have been recently described in the literature. Most of these methods require knowing strain energy distribution for the undamaged structure (baseline SEMS). This is especially true for detection of small damages, where changes in the SEMS cannot be observed otherwise. Usually, the mode shapes from the structure under test should be compared to the baseline mode shapes to provide sufficient data for damage detection. However, these methods do not cover damage detection on structures where baseline mode shapes cannot be readily obtained, for example, structures with preexisting damage. Conventional methods, like building a finite element (FE) model of a structure to be used as a baseline might be an expensive and time-consuming task that can be impossible for complex structures. This paper suggests a method for extraction of localized changes (damage peaks) from SEMS based on Fourier analysis of the strain energy distribution. A detailed analytical proof is given for the case of a pinned–pinned beam and a numerical proof for the free–free beam. The analytical predictions have been confirmed both by the FE model and impact testing experiments on a free–free aluminum beam, including single and multiple damage scenarios.

Keywords: Strain energy mode shapes; Non-destructive damage detection; Free–free aluminum beam; Pinned–pinned beam

INTRODUCTION

In the recent past, several methods for detecting and locating damage (usually cracks) from changes in strain energy mode shapes (SEMS) have been developed. Methods employing curvature mode shapes represent a very similar approach. All these methods attempt to detect and locate damage that produces localized changes in elastic modulus without significant changes in mass. Such damage can be observed as localized changes (damage peaks) on SEMS.

The majority of these methods requires knowing strain energy distribution (mode shapes) for the structure without any damage or so-called baseline SEMS. The comparison to

*Corresponding author. E-mail: esazonov@csee.wvu.edu

NON-BASELINE DETECTION OF SMALL DAMAGES FROM CHANGES IN STRAIN ENERGY MODE SHAPES

Edward S. Sazonov, Powsiri Klinkhachorn, Udaya B. Halabe and Hota V.S. GangaRao

ABSTRACT

Several methods for damage detection based on identifying changes in strain energy mode shapes have been recently described in the literature. Most of these methods require knowing strain energy distribution for the undamaged structure (baseline strain energy mode shapes). This is especially true for detection of small damages, where changes in the strain energy mode shapes cannot be observed otherwise. Usually, the mode shapes from the structure under test should be compared to the baseline mode shapes to provide sufficient data for damage detection. However, these methods do not cover damage detection on structures where baseline mode shapes cannot be readily obtained, for example, structures with preexisting damage. Conventional methods, like building a finite element model of a structure to be used as a baseline might be an expensive and time-consuming task that can be impossible for complex structures. This paper suggests a method for extraction of localized changes (damage peaks) from strain energy mode shapes based on Fourier analysis of the strain energy distribution. A detailed analytical proof is given for the case of a pinned-pinned beam and a numerical proof for the free-free beam. The analytical predictions have been confirmed both by the finite element model and impact testing experiments on a free-free aluminum beam, including single and multiple damage scenarios.

KEYWORDS: strain energy mode shapes, non-destructive damage detection

1. INTRODUCTION

In the recent past, several methods for detecting and locating damage (usually cracks) from changes in Strain Energy Mode Shapes (SEMS) have been developed. Methods employing curvature mode shapes represent a very similar approach. All these methods attempt to detect and locate damage that produces localized changes in elastic modulus without significant changes in mass. Such damage can be observed as localized changes (damage peaks) on strain energy mode shapes.

The majority of these methods requires knowing strain energy distribution (mode shapes) for the structure without any damage or so-called baseline SEMS. The comparison to the baseline is used to enhance appearance of damage peaks that sometimes may not be observed otherwise. The need for baseline SEMS is especially obvious for identifying small damages that produce very subtle changes in SEMS.

Unfortunately, such an approach often is not feasible for a class of structures where undamaged state is unknown and cannot be acquired experimentally. This class of structures primarily includes old structures where damage state is unknown but the need for non-destructive testing is usually greater. Conventional methods, such as building a Finite Element (FE) model of a structure may represent a tedious, expensive and time-consuming task. Besides, it is difficult or sometimes impossible to reach required accuracy of mode shape approximation by a FE model.

If applicability of non-destructive damage detection utilizing SEMS could be extended by eliminating the need for baseline mode shapes and employing a non-baseline approach, it would significantly increase the class of structures where non-destructive damage detection could be performed.

Consider some of the recent work in this area. Pandey et. al. [1] detected crack location by identifying changes in curvature mode shapes. The crack location was established by comparing curvature mode shapes of the structure under test to baseline mode shapes. Shi et.al. [2] suggested using changes in strain energy distribution to detect and localize damage. The recommended method monitors changes in

modal strain energy in each structural element comparing the states before and after it was damaged. Therefore, this methodology also makes use of a baseline. Ratcliff and Hoerst [3, 4] introduced a modified Laplacian operator for damage detection from the mode shape data. This work made an effort to introduce a non-baseline approach and claimed that it “does not require *a-priori* knowledge of the undamaged structure”. Enhancing appearance of the damage peaks for small damages was performed by fitting a cubic polynomial to the mode shapes obtained from the structure under test and using this polynomial fit as a baseline. At the same time the author did not provide the groundwork for approximating the baseline in such a manner and suggested a trial-and-error approach. Farrar and Jauregui [5] conducted a comparative study of different damage identification algorithms on a bridge. The curvature-based methods performed very well compared to other methods tested in the experiments, occupying the top two places by the accuracy of detection. The authors also noted the methods’ high sensitivity to less severe damage cases. Osegueda, Carrasco and Meza [6] investigated strain energy method on aluminum cantilever beams and honeycomb composite plates. The authors received positive damage detection results in experiments with beams and negative results in experiments with composite plates. They also claimed that strain energy methods not only can identify damage but also quantify it by accounting the energy relations between damaged and undamaged states. Cornwell et. al. [7] performed a comparative study of two vibration-based damage identification algorithms, including strain energy method. The testing was conducted on a beam and a plate, comparing the damaged vs. undamaged strain energy distribution. Strain energy method successfully identified severe damage cases, but a masking effect was reported for lower level damages, i.e. when the two damage locations had different levels of damage, the algorithm tended to only conclusively identify the location with the largest amount of damage. Wahab and Roeck [8] used modal curvatures for detecting damage in bridges using the change in dynamic parameters between the intact and damage states. The same paper also introduced a damage indicator called “curvature damage factor” in which the difference in curvature mode shapes for all modes

can be summarized in one number for each measurement point. Yoo, Kwak and Kim [9] used difference in strain energy mode shapes between damaged and undamaged cases to detect and locate damage in a plate. Yan and Deng [10] applied the strain energy algorithm to nondestructive damage detection in bridges. They conducted numerical experiments on a finite element model of a freely supported bridge T-beam. Pereyra et. al. [11] studied damage detection in an aluminum stiffened-plate panel resembling aircraft fuselage construction. As in most other studies, the damaged strain energy mode shapes were compared to the undamaged strain energy mode shapes. Statistical methods were employed to jointly analyze information from several mode shapes and to locate damage. Napolitano [12] investigated quality of damage detection using reduced measurements and the strain energy algorithm. The author concluded that the strain energy method performs better when many response points are measured. Cornwell, Doebling and Farrar [13] provided a detailed theoretical explanation on application of the strain energy method to plate-like structures. They reported that the method was effective enough to detect areas with 10% reduction in stiffness.

A method based on strain energy mode shapes was developed at West Virginia University (WVU) [14, 15]. Strain energy for an interval $[a,b]$ was computed using the following formula:

$$U_{[a,b]} = \frac{1}{2} \int_a^b EI(\Phi'')^2 dx \quad (1)$$

where

EI = flexural stiffness of the cross-section;

Φ = mode shape vector (displacement mode shape).

Subtracting the baseline SEMS from the SEMS acquired from the structure under test produces so-called Difference Strain Energy Mode Shapes (DSEMS) where crack locations are identified as damage peaks. Again, this method requires a baseline to extract and enhance appearance of damage peaks.

This paper attempts to extend the WVU method and eliminate the usage of baseline mode shapes in the damage detection process. The suggested procedure performs extraction and enhancement of damage peaks appearance through separation of damage information in frequency domain rather than traditional spatial domain. An example of comparative spectral analysis is given for a case of a pinned-pinned beam and for a beam with free-free boundary conditions (both with uniform cross-section). The results of the analysis show that the amplitude spectra of the strain energy mode shapes are band-limited to the first few harmonics, while amplitude spectrum of a crack is significantly wider. Thus, the damage introduced into the structure creates additional harmonics in the amplitude spectrum of the strain energy mode shapes that have not been present in the undamaged beam. These additional harmonics can be extracted by filtering and restored to produce enhanced damage peaks. The analytical results are confirmed both by FE model and impact testing experiments.

2. AMPLITUDE SPECTRUM OF SEMS FOR DAMAGED AND UNDAMAGED STRUCTURES

2.1 Amplitude Spectrum of SEMS of a Pinned-Pinned Beam

Consider an undamaged pinned-pinned beam of length L and a uniform cross-section with the flexural stiffness of EI . The bending mode shapes of the beam can be determined using simple Euler-Bernoulli pure flexure model:

$$EI \frac{\partial^4 y}{\partial x^4} = -m \frac{\partial^2 y}{\partial t^2}, \quad (2a)$$

where x is the distance measured along the length of the beam, y is the vertical deflection, and m is the mass per unit length of the beam.

The general form of the solution for the equation (2a) is:

$$\begin{aligned}
y(x,t) &= \Phi(x)\theta(t) \\
&= [A \cosh \lambda x + B \sinh \lambda x + C \cos \lambda x + D \sin \lambda x] [E \cos \alpha \lambda^2 t + F \sin \alpha \lambda^2 t],
\end{aligned} \tag{2b}$$

where $\alpha^2 = \frac{EI}{m}$ and λ is the eigenvalue to be determined from the boundary conditions. Particular

solutions for a variety of the boundary conditions can be found in [16]. For a pinned-pinned beam, displacement mode shapes for mode k are given by the following equation:

$$\Phi_k(x) = A_k \sin\left(\frac{\pi k}{L} x\right) = A_k \sin\left(\frac{\omega_k}{2} x\right) \tag{2c}$$

where A_k = amplitude of mode k ;

$\omega_k = \frac{2\pi k}{L}$ - angular frequency for mode shape k .

Thus, the strain energy in interval $[a,b]$ for mode k of a pinned-pinned beam can be computed from (1) and (2c):

$$U_{[a,b]} = \frac{1}{2} \int_a^b EI \left(\frac{d^2 A_k \sin\left(\frac{\omega_k}{2} x\right)}{dx^2} \right)^2 dx = C_k \int_a^b \sin^2\left(\frac{\omega_k}{2} x\right) dx \tag{3}$$

where $C_k = \frac{EIA_k^2 \omega_k^4}{32}$.

For the next step, a formula for computing strain energy mode shape as a function of x (location) may be derived by utilizing the mean value theorem of a definite integral:

$$\int_a^b f(z) dz = f(\xi)(b-a) \quad \text{where } a < \xi < b.$$

Therefore, for a sampling interval $\Delta = b - a = \text{const}$; $\Delta \ll L$; $\xi \approx x = \frac{a+b}{2}$ the strain energy

mode shape for mode k can be expressed as:

$$U_k(x) \approx C_k \Delta \sin^2\left(\frac{\omega_k}{2}x\right) \quad (4)$$

The properties of the frequency spectrum of the strain energy mode shapes can be established by applying Fourier series to the equation (4). The general form of the Fourier series is:

$$f(x) = A_0 + \sum_{n=1}^{\infty} A_n \sin \omega_n x + \sum_{n=1}^{\infty} B_n \cos \omega_n x \quad (5)$$

The A_0 component for mode k is:

$$A_0^k = \frac{1}{L} \int_0^L C_k \Delta \sin^2\left(\frac{\omega_k}{2}x\right) dx = \frac{C_k \Delta}{2}$$

A periodic extension of function $U_k(x)$ is even, therefore only cosine coefficients of the Fourier series should be computed. Taking into account that circular frequency of the n -th harmonic

is $\omega_n = \frac{2\pi n}{L}$, the Fourier coefficients for mode k and harmonic n are as follows:

$$\begin{aligned} B_n^k &= \frac{2}{L} \int_0^L C_k \Delta \sin^2\left(\frac{\omega_k}{2}x\right) \cos(\omega_n x) dx = \\ &= \frac{C_k \Delta}{L} \left(\frac{L}{2\pi n} \sin\left(\frac{2\pi n}{L}x\right) \right) \Big|_0^L - \frac{C_k \Delta}{2L} \left(\frac{L}{2\pi(k-n)} \sin\left(\frac{2\pi(k-n)}{L}x\right) + \frac{L}{2\pi(k+n)} \sin\left(\frac{2\pi(k+n)}{L}x\right) \right) \Big|_0^L \\ &= 0 \end{aligned}$$

$B_n^k = 0$ for every $n \neq k$. In case $n=k$ there is a singularity that should be resolved.

$$B_k^k = \lim_{k \rightarrow n} \left[-\frac{C_k \Delta}{2L} \left(\frac{L}{2\pi(k-n)} \sin\left(\frac{2\pi(k-n)}{L}x\right) \right) \Big|_0^L \right] = -\frac{C_k \Delta}{2} \lim_{\theta \rightarrow 0} \frac{\sin \theta}{\theta} = -\frac{C_k \Delta}{2},$$

where $\theta = 2\pi(k-n)$.

Thus, the Fourier series for $U_k(x)$ consists only of two members for any mode k .

$$U_k(x) = \frac{C_k \Delta}{2} - \frac{C_k \Delta}{2} \cos \omega_k x = \frac{C_k \Delta}{2} (1 - \cos \omega_k x)$$

It is more convenient to represent Fourier series in the amplitude-phase spectrum form:

$$f(x) = A_0 + \sum_{n=1}^{\infty} \bar{A}_n \sin(\omega_n x + \varphi_n) \quad (6)$$

where

$$\bar{A}_n = (A_n^2 + B_n^2)^{\frac{1}{2}}; \tan \varphi_n = \frac{B_n}{A_n}.$$

Amplitude spectra of the strain energy mode shapes for the first five modes of a pinned-pinned beam are given on Figure 1. Amplitude of harmonics for FE model is normalized with respect to the value of A_0 . The most important implication is that the spectra of strain energy mode shapes are band-limited to a few lower harmonics carrying most of the mode shapes' energy. From the practical point of view a cut-off limit can be established, equal, for example, to the highest harmonic bounding 95% of a mode shape's energy.

2.2 Amplitude Spectrum of SEMS of a Free-Free Beam

Simulating the free-free boundary conditions by suspending the structure on elastic cords or by supporting the structure on airbags is a common practice in application of the method of strain energy mode shapes. Thus, it would also be useful to conduct analysis of the spectral properties of the strain energy mode shapes for a free-free beam. The analysis of a beam with free-free boundary conditions is very similar to the analysis performed for the case of a pinned-pinned beam.

Displacement mode shapes for mode k are given by the following equation [16]:

$$\Phi_k(x) = \cosh\left(\frac{\lambda_k x}{L}\right) + \cos\left(\frac{\lambda_k x}{L}\right) - \sigma_k \left(\sinh\left(\frac{\lambda_k x}{L}\right) + \sin\left(\frac{\lambda_k x}{L}\right) \right) \quad (7)$$

where L – length of the beam;

λ_k and σ_k - mode shape coefficients dependent on k :

$$\lambda_k = \{ 4.730040739999998, 7.853204619999998, 10.9956078, 14.1371655, \\ 17.278759699999999, (2k+1)\pi/2 \text{ for } k>5\};$$

$$\sigma_k = \frac{\cosh \lambda_k - \cos \lambda_k}{\sinh \lambda_k - \sin \lambda_k}.$$

Utilizing the same approach as in (3) and (4), the strain energy mode shapes are:

$$U_k(x) \approx \frac{1}{2} \Delta \left(-\frac{\lambda_k^2 \cos(\frac{\lambda_k x}{L})}{L^2} + \frac{\lambda_k^2 \cosh(\frac{\lambda_k x}{L})}{L^2} - \sigma_k \left(-\frac{\lambda_k^2 \sin(\frac{\lambda_k x}{L})}{L^2} + \frac{\lambda_k^2 \sinh(\frac{\lambda_k x}{L})}{L^2} \right) \right)^2 \quad (8)$$

Analytical application of the Fourier transform to (8) is rather complicated, whereas a numerical approach is more appropriate and easy. The $U_k(x)$ has been discretized into an array with 100 elements and Discrete Fourier Transform (DFT) performed with subsequent computation of the amplitude spectrum. Figure 1 shows the amplitude spectra of the SEMS for the first five modes of a free-free beam. Results from the numeric experiment have been complemented by the results obtained on a FE model (which is described later).

Total energy of the signal is contained within 50 harmonics (after DFT of a 100-point signal). A cut-off frequency has been established for each mode of vibration at the harmonic that limits the signal's energy at 95% of total energy (Table I). As it can be observed from the data, the cut-off harmonic $n_{Cut-off}$ has a well-defined dependency on k :

$$n_{Cut-off} = k + 1 \quad (9)$$

Thus, the amplitude spectrum of SEMS for a beam with free-free boundary conditions is band-limited by the $k+1$ harmonic.

2.3 Amplitude Spectrum of a Damage Peak

The analysis conducted in sections 2.1 and 2.2 established that the amplitude spectra of the strain energy mode shapes for pinned-pinned and free-free beams is band-limited for the first k and $k+1$ harmonics, respectively. The goal of this section is to show that the amplitude spectrum of a damage peak is significantly wider than the amplitude spectrum of an undamaged strain energy mode shape. Although a precise analytical or numerical solution for a crack-like type of damage is theoretically possible, a simplified model of the damage was accepted to illustrate the principle of the suggested methodology. The suggested model of a damage as a rectangular pulse corresponds really well to the experimental results [2, 5, 6, 14, 15] and simplifies the analysis. Furthermore, the shape of the pulse is not as important as it's relative width to the length of the beam. Indeed, if the width of a damage peak l is significantly smaller than the length of the structure L then the amplitude spectrum of the peak will be significantly wider than the amplitude spectrum of the baseline mode shapes.

Consider effects of a damage (crack) on strain energy mode shapes: first, the amplitude of a mode shape decreases due to the relaxation of the structure (changes in the shape can be neglected for small damages); second, localized changes in the shape (a damage peak) appear at the place of damage location. These effects can be expressed in the following manner:

$$\bar{U}_k(x) = \alpha U_k(x) + d(x) \quad (10)$$

where

$\bar{U}_k(x)$ = strain energy mode shape for a damaged structure;

$U_k(x)$ = strain energy mode shape for the undamaged structure;

α = a coefficient reflecting reduction in the amplitude ($0 \leq \alpha \leq 1$);

$d(x)$ = a function representing the damage peak.

The traditional process of extracting damage peaks from the strain energy mode shapes for a structure under test includes subtracting the baseline mode shapes from the test mode shapes. According to (10) this process generates a small error that is present on resulting difference strain energy mode shapes:

$$e_k(x) = \bar{U}_k(x) - U_k(x) = \alpha U_k(x) + d(x) - U_k(x) = (\alpha - 1)U_k(x) + d(x)$$

For the sake of spectral analysis, function $d(x)$ can be approximated as a rectangular pulse (Figure 2). In general, width of a peak is significantly less than length of structure ($l \ll L$) and it can be located anywhere along structure's length. Consider the frequency properties of the peak from Figure 2:

$$A_0 = \frac{1}{L} \int_0^L d(x) dx = \frac{h}{L} x \Big|_0^l = \frac{hl}{L}$$

$$B_n = \frac{2}{L} \int_0^L d(x) \sin(\omega_n x) dx = \frac{2h}{L} \left(-\frac{1}{\omega_n} \cos(\omega_n x) \Big|_0^l \right) = \frac{h}{\pi n} \left(1 - \cos\left(\frac{2\pi n l}{L}\right) \right) \quad (11)$$

Unlike the spectrum of a strain energy mode shape for the discussed boundary conditions, the spectrum of a damage peak is not limited to a certain number of harmonics but extends to infinity. The amplitude spectrum of a damage peak can be computed using the following formula:

$$\bar{A}_n = \frac{h}{\pi n} \left(1 - \cos\left(\frac{2\pi n l}{L}\right) \right) \quad (12)$$

For any $l \ll L$ the first zero node is reached at $n \approx \frac{L}{l}$ and $n \gg 1$. The first 40 harmonics of the amplitude spectrum of a damage peak with amplitude $h=1$ and $L=20l$ are given in Figure 3. According to the translation properties of the Fourier transform:

$$d(x - x_0) \Leftrightarrow |D(n)| e^{\frac{-j2\pi nx_0}{L}} \quad (13)$$

Therefore, any function $d(x)$ will have the same amplitude spectrum (given that all $d(x)$ have the same shape and amplitude) but different phase spectrum.

3. EXTRACTING DAMAGE PEAKS IN THE FREQUENCY DOMAIN

The following important characteristics of strain energy mode shapes have been established during analysis:

1. Undamaged strain energy mode shapes have amplitude spectrum limited by the k harmonic (where k is the mode number) for the pinned-pinned beam and by the $k+1$ harmonic for the free-free beam.
2. The amplitude spectrum of a damage peak extends to infinity.
3. The normalized amplitude spectrum for a damage peak at any location is equal to amplitude spectrum of a damage peak at any other location (given the assumption that all damage peaks have the same shape and amplitude).

These characteristics suggest that it might be possible to separate mode shape information from damage information in the frequency domain and thus avoid usage of a baseline.

Consider a modified version of equation (10): a strain energy mode shape for a damaged structure represented as a sum of the mode shape function $\alpha U_k(x)$ for undamaged structure and one or several functions $d(x)$.

$$\bar{U}_k(x) = \alpha U_k(x) + d_1(x) + \dots + d_i(x) \quad (14)$$

Ideally, a damage extraction procedure should remove mode shape component $\alpha U_k(x)$ and leave damage response $r(x) = d_1(x) + \dots + d_i(x)$ intact. One way to perform such an operation is to know a good approximation of $\alpha U_k(x)$. This tactic is used in the baseline detection. Another approach would be to consider properties of $\bar{U}_k(x)$ in the frequency domain. Indeed, a Fourier transform of $\bar{U}_k(x)$ would have the following form:

$$\bar{U}_k(n) = \alpha U_k(n) + D_1(n) + \dots + D_i(n) \quad (15)$$

From the previous section it is known that $U_k(n) = 0$ for any $n > k+1$ ($k+1$ covers both pinned-pinned and free-free boundary conditions) and $D_i(n) \neq 0$ for any $n \neq \frac{L}{l}$. Therefore, components $U_k(n)$ and $D_1(n) \dots D_i(n)$ intersect only in the lower part of the spectrum and do not intersect for all $n > k+1$ (higher part of the spectrum). The suggested damage extraction procedure attempts to eliminate component $\alpha U_k(n)$ and respectively $\alpha U_k(x)$ by removing the first several harmonics of the amplitude spectrum. The only parameter to be used for such procedure is the highest non-zero harmonic of $U_k(x)$ which in this case is equal to $k+1$. Consider the effect of removing $\alpha U_k(n)$ from $\bar{U}_k(x)$ in the assumption that $\alpha U_k(n)$ has M non-zero harmonics in the amplitude spectrum and the total spectrum consists of $\frac{N}{2}$ harmonics, where $\frac{N}{2} > M$ and $\frac{N}{2}$ is large enough to accommodate most of the signal's energy. Then (15) can be represented as:

$$\bar{U}_k(n) = \alpha U_k(0) + \dots + \alpha U_k(M-1) + D_1(0) + \dots + D_1\left(\frac{N}{2}-1\right) + \dots + D_i(0) + \dots + D_i\left(\frac{N}{2}-1\right)$$

In order to eliminate $\alpha U_k(n)$, values of $\alpha U_k(0) \dots \alpha U_k(M-1)$ should be set to zero. This would only be possible if the first M values of $D_1(n) \dots D_i(n)$ were also set to zero. Such an operation would introduce some error $e(n)$ into $D_1(n) \dots D_i(n)$:

$$R(n) = \hat{R}(n) + e(n) \quad (16)$$

where

$$R(n) = \text{DFT of the damage response function } r(x) = d_1(x) + \dots + d_i(x);$$

$$\hat{R}(n) = D_1(M) + \dots + D_1\left(\frac{N}{2} - 1\right) + \dots + D_i(M) + \dots + D_i\left(\frac{N}{2} - 1\right) = \text{damage response function}$$

extracted by the amplitude spectrum modification;

$$e(n) = D_1(0) + \dots + D_1(M-1) + \dots + D_i(0) + \dots + D_i(M-1) = \text{error.}$$

As it follows from (16) the resulting error is proportional to the number of frequency bins occupied by $\alpha U_k(n)$ and therefore, to the mode number k . In regard to this property, the error is the lowest for the first mode and it grows with the mode number. The error also depends on values of $D_1(n) \dots D_i(n)$ at the first M frequency bins and the quantity i of functions D . The function $\hat{r}(x)$ obtained by applying inverse DFT to $\hat{R}(n)$ will be different from the “ideal” damage response $r(x)$. Although it is impossible to make a precise estimate as to how this difference will affect the shape of $\hat{r}(x)$, the following observations could provide the general guidelines:

1. “Sharp” points of damage peaks are represented by the higher frequencies of the spectrum, therefore suggested spectrum modification will not influence them.
2. Only the amplitude spectrum of the strain energy mode shapes is modified, therefore the damage peaks will not change their locations.

3. Improvement in the appearance of $d_1(x) \dots d_i(x)$ after spectrum modification can be connected to a measure of energy: if $|e(n)|^2 < |\alpha U_k(n)|^2$ then appearance of damage response should improve. Considering the fact that for small damages the energy contained in $r(x)$ is significantly lower than the energy in $\alpha U_k(x)$, this inequality should generally be true.
4. It is hard to compare errors occurring during baseline and non-baseline damage peak extraction. In the first case, the error is mainly proportional to the relaxation of the structure and is a function of $U_k(x)$, in the second case the error is both a function of $U_k(x)$ and $d_1(x) \dots d_i(x)$. However, practical observations show that baseline extraction provides slightly better results.

4. TESTING ON A FREE-FREE ALUMINUM BEAM

The suggested procedure has been tested both on FE and experimental data. The first set of experiments was conducted on FE model of a free-free beam that provided an almost noise-free environment for testing. Dimensions and other parameters of the FE model are shown on Figure 4. The model is consistent with the aluminum beam later used in impact testing experiments. Cracks were modeled by removing elements; removing a single element was equivalent to inflicting 12.5% reduction in cross-section. The first five strain energy mode shapes for a damage at location 22 are shown in Figure 5. As it can be observed from the Figure 5, only mode 1 and mode 2 have visible damage peaks, and the amplitude of the damage peaks is very low compared to the amplitude of the strain energy mode shapes. The vertical axis is simply marked "Value" due to the fact that the outcome of the numeric strain energy processing and consequent spectrum modification does not have any sensible physical meaning, but rather has its importance in the relative position of each point in a mode shape. A set of rectangular filters was

applied to the strain energy mode shapes in order to extract damage peaks. The filters were produced using the following formula:

$$F_k(n) = \begin{cases} 0, & \text{if } n \leq k+1 \\ 1, & \text{if } n > k+1 \end{cases}, 0 \leq n \leq \frac{N}{2} - 1 \quad (17)$$

The strain energy mode shapes after spectrum modification are shown in Figure 6. The Modified Spectrum Strain Energy Mode Shapes (MSSEMS) have distinct peaks at the location of damage in all of the five modes.

The impact testing experiments were conducted on a free-free aluminum beam (suspended on elastic cords during the experimentation) with 12.7mm x 25.4mm x 762mm (0.5”x1”x30”) dimensions (same as the FE model). The vibration data were acquired using an impact hammer utilizing the standard procedure [15]. The total scan consisted of 27 spatial points. The data acquisition for each point was performed only once, therefore there was a significant amount of noise present in the mode shapes. This noise created additional obstacles for damage peak extraction. The measured data were interpolated by cubic splines to enhance resolution up to 61 points used in the FE model experiments. Two cracks were simulated by inflicting 6.35 mm (¼”) cuts at locations 38 and 47. Unlike the FE model, vibration data were obtained for the first six modes but frequency limitations of the accelerometer made the first mode readings absolutely unreliable. Thus, only modes from two to six could actually be used for in damage detection. Figure 7 shows the difference strain energy mode shapes for this test case. Figure 8 shows the MSSEMS, so that the quality of the non-baseline procedure can be compared to the baseline detection. As it can be seen, there is no significant difference in the quality of the waveforms. In order to provide a better comparison, both DSEMS and MSSEMS were processed by an automated fuzzy expert system [17] whose sole purpose is to identify damage on strain energy mode shapes (obtained by the traditional baseline method). The fuzzy expert system detects damage by analyzing the magnitude, location and other parameters of damage peaks and comparing those parameters in peaks across modes. The automated

damage detection procedure utilizes the expert knowledge to facilitate damage detection and fuzzy logic to deal with the uncertainties of the task. Results from the fuzzy expert system supply an indirect indication that the suggested method provides the quality of damage peak extraction comparable to those of the traditional method. Figure 9 illustrates the results of the automated damage detection: both data sets provided sufficient data for reliable recognition of both damage locations.

6. CONCLUSIONS

The method presented in this paper can be applied to beams without a known baseline, thus extending applicability of the damage detection by strain energy mode shapes. The analytical and numerical proof of the method has been confirmed by experiments conducted on a simple aluminum beam. The suggested non-baseline approach was successful in detecting and localizing cracks. The quality of damage peak extraction was sufficient to observe localized changes in SEMS as a result of relatively small damages (12.5% cross-sectional reduction). The method's performance is expected to be even better for larger damages. In general, the method was sufficiently effective and robust to detect both single and multiple damages in conditions with or without noise and with no knowledge of baseline mode shapes.

Although the free-free and pinned-pinned boundary conditions were of the primary interest, it seems possible to extend the method to other boundary conditions, although this might require additional theoretical work due to the fact that those boundary conditions may not have so well-defined spectral limits.

ACKNOWLEDGEMENTS

The authors wish to acknowledge the financial support provided by the U.S. Army (contract # DAAE07-96-C-X226).

REFERENCES

1. Pandey A.K., Biswas M., Samman M.M. (1991). "Damage detection from changes in curvature mode shapes". *Journal of Sound and Vibration*, vol. 145, n.2, pp. 321-332
2. Shi Z.Y., Law S.S., Zhang L.M. (1998). "Structural damage localization from modal strain energy change". *Journal of Sound and Vibration*, vol. 218, n.5, pp. 825-844
3. Ratcliffe C.P. (1997). "Damage detection using a modified Laplacian operator on mode shape data". *Journal of Sound and Vibration*, vol. 204, n.3, pp.505-517
4. Hoerst B., Ratcliff C.P. (1997). "Damage detection in beams using Laplacian operators on experimental modal data", *Proceedings of International Modal Analysis Conference (IMAC-XV)*, Orlando, Florida, pp. 1305-1311
5. Farrar C.R., Jauregui D.A. (1998). "Comparative study of damage identification algorithms applied to a bridge", *Smart Materials and Structures*, n.7, pp. 704-719
6. Osegueda R.A., Carrasco C.J., Meza R. (1997). "A modal strain energy distribution method to localize and quantify damage", *Proceedings of International Modal Analysis Conference (IMAC-XV)*, Orlando, Florida, pp. 1298-1304
7. Cornwell P., Kam M., Carlson B., Hoerst B., Doebling S., Farrar C. (1998). "Comparative study of vibration-based damage ID algorithms", *Proceedings of International Modal Analysis Conference (IMAC-XVI)*, Santa-Barbara, California, pp. 1710-1716
8. Wahab A., Roeck G., "Damage detection in bridges using modal curvatures: application to a real damage scenario", *Journal of Sound and Vibration*, v.226, n.2, pp. 217-235
9. Yoo S.H., Kwak H.K., Kim B.S. (1999). "Detection and location of a crack in a plate using modal analysis", *Proceedings of International Modal Analysis Conference (IMAC-XVII)*, Orlando, Florida, pp. 1902-1908

10. Yan P., Deng Y. (2000). "Nondestructive damage detection of bridges based on strain mode", Proceedings of International Modal Analysis Conference (IMAC-XVIII), San-Antonio, Texas, pp. 1825-1830
11. Pereyra L., Osegueda R., Carrasco C., Ferregut C. (2000). "Detection of damage in a stiffened plate from fusion of modal strain energy differences", Proceedings of International Modal Analysis Conference (IMAC-XVIII), San-Antonio, Texas, pp. 1556-1562
12. Napolitano K., "Damage detection using reduced measurements: analytical investigation", retrieved from http://casl.ucsd.edu/casl/abstracts/abstract_damage_detect_ai.htm
13. Cornwell P., Doebling S., Farrar C., "Application of the strain energy damage detection method to plate-like structures", Journal of Sound and Vibration, v.224, n.2, pp.359-374
14. S.H.Petro, S.E.Chen, H.V.S. GangaRao (1997). "Damage Detection Using Vibration Measurements," Proceedings, 15th IMAC, Orlando FL, pp.113-127
15. S. Venkatappa (1997). Damage Detection Using Vibration Measurements, M.S. Thesis submitted to West Virginia University.
16. R. Blevins (1979), "Formulas for natural frequency and mode shape", Van Nostrand Reinhold Company.
17. E. S. Sazonov, P. Klinkhachorn, H. V. S. GangaRao, U. B. Halabe, "Fuzzy Logic Expert System for Automated Damage Detection from Changes in Strain Energy Mode Shapes", submitted for publication to Nondestructive Testing and Evaluation

Table I. Percentage of total energy contained within first 10 harmonics (free-free case).

Mode	Frequency bins									
	0	0-1	0-2	0-3	0-4	0-5	0-6	0-7	0-8	0-9
1	55.82	91.86	99.43	99.9	99.97	99.99	99.99	99.99	99.99	99.99
2	51.3	61.66	88.47	98.56	99.64	99.89	99.96	99.98	99.99	99.99
3	48.49	52.61	64.51	86.36	97.72	99.31	99.74	99.89	99.95	99.97
4	46.53	48.69	55.17	65.86	84.89	97	98.95	99.57	99.8	99.9
5	45.07	46.42	50.3	57.2	66.64	83.79	96.39	98.62	99.62	99.7

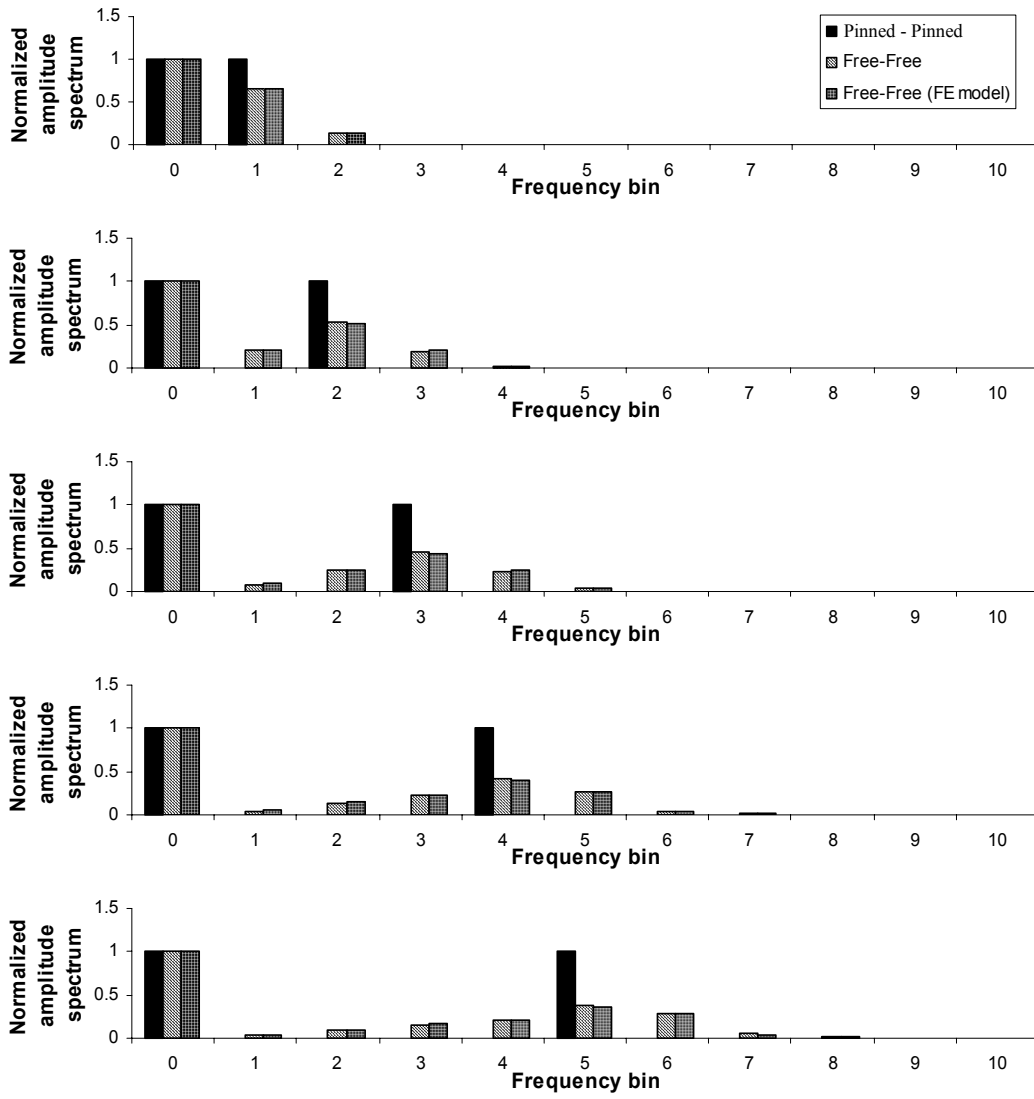


Figure 1. Amplitude spectra of strain energy mode shapes for the first five vibration modes of a beam.

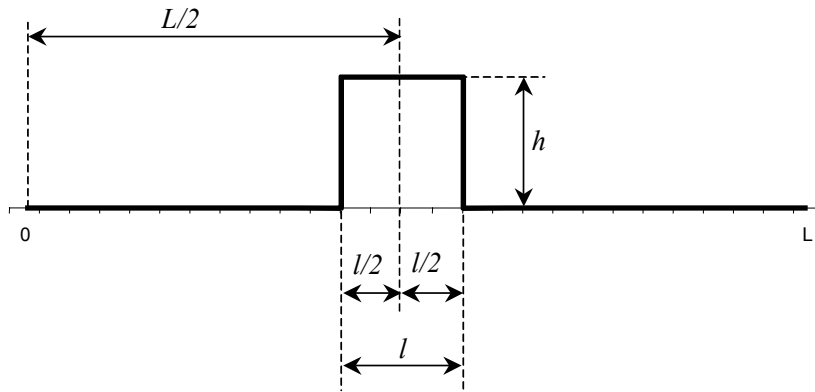


Figure 2. Approximation of a damage peak.

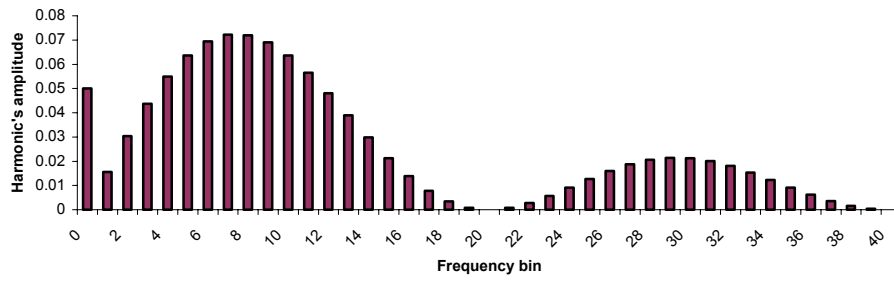


Figure 3. Amplitude spectrum of a damage peak.

Modeling software: ALGOR;
Element dimensions: 3.2 mm × 12.7 mm × 3.2 mm;

Element type: plate;
Number of nodes: 241 × 9.

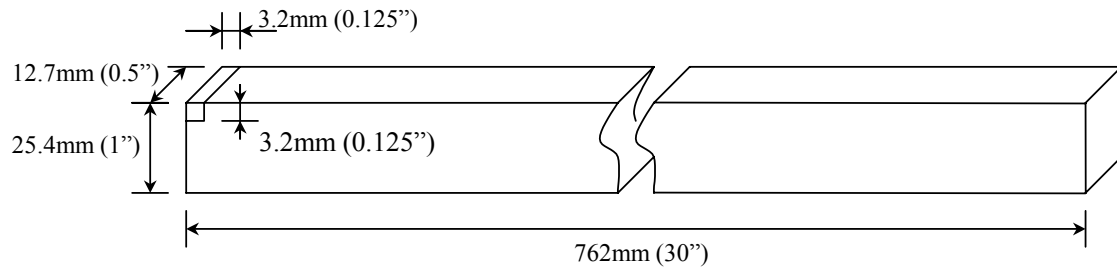


Figure 4. FE model of a pinned-pinned beam.

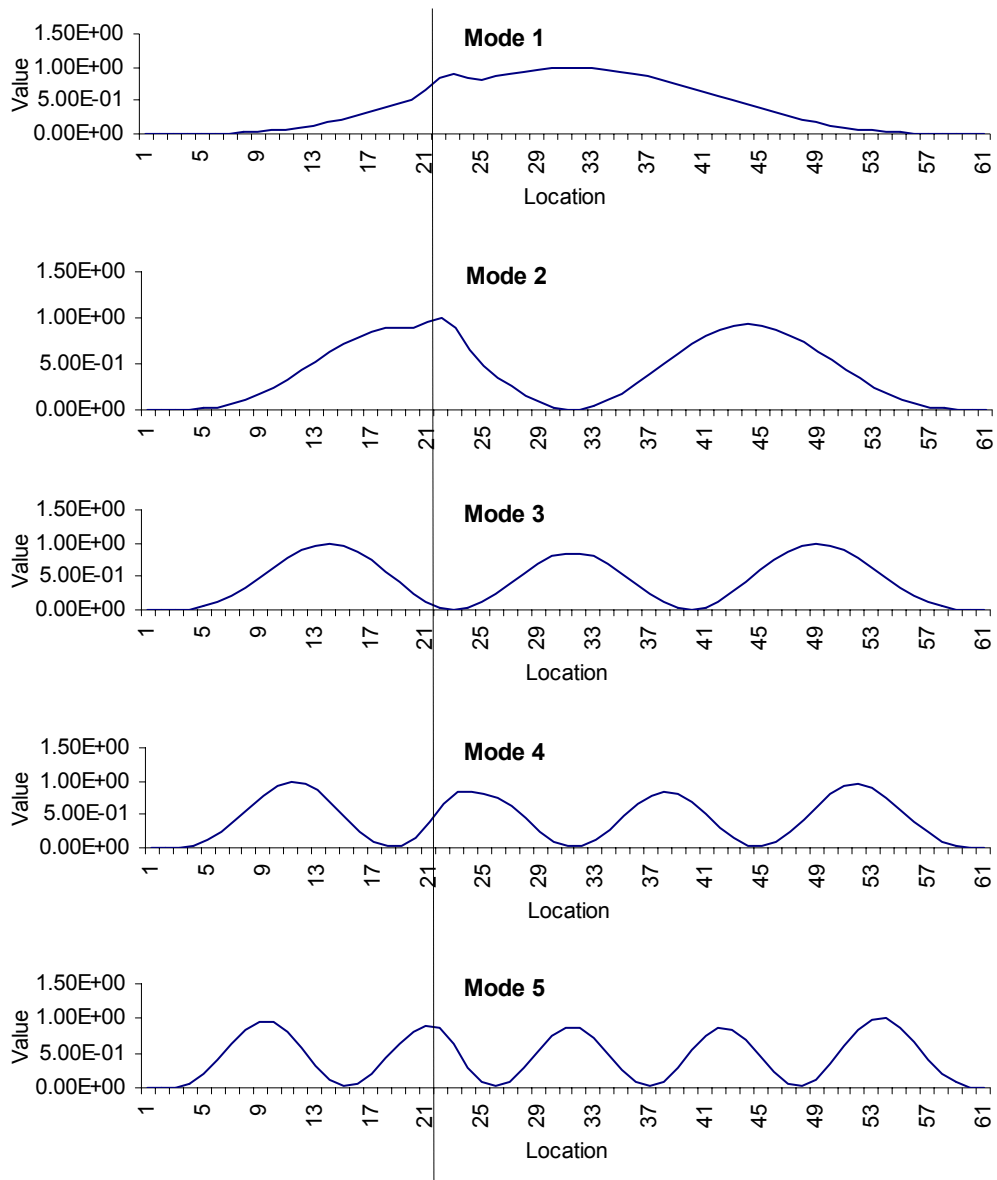


Figure 5. Strain energy mode shapes for the FE experiment. Damage at location 22.

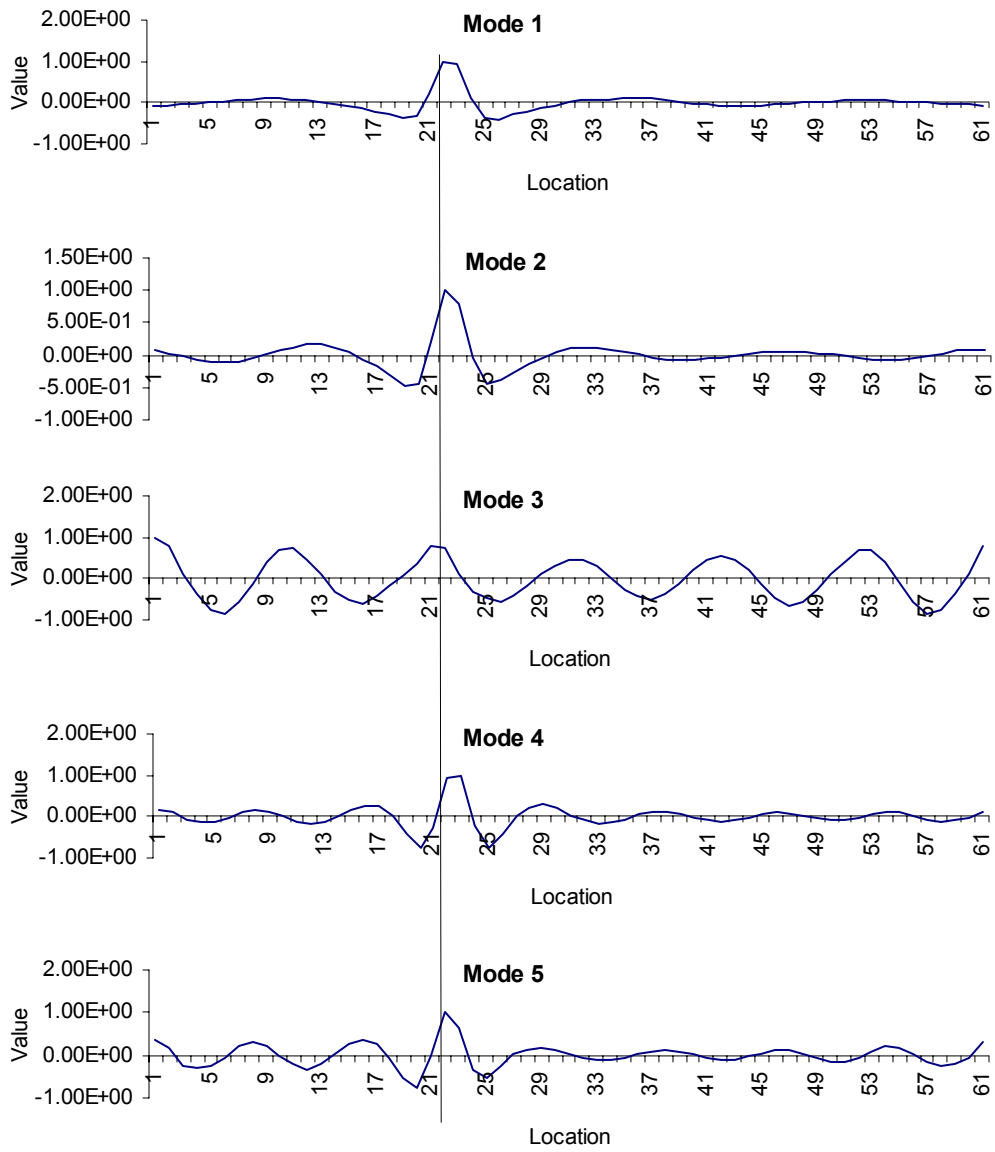


Figure 6. Strain energy mode shapes for the FE experiment after spectrum modification. Damage at location 22.

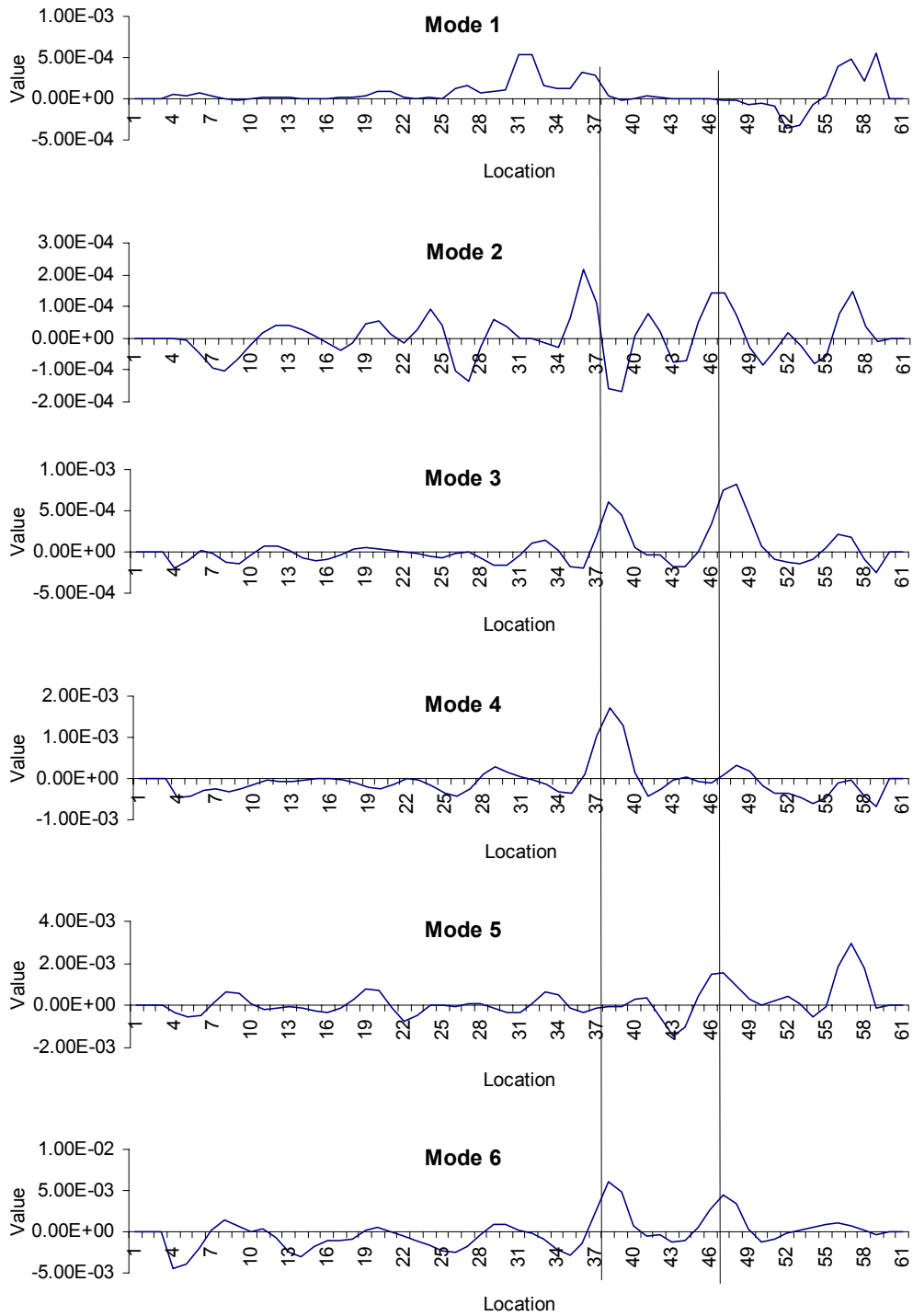


Figure 7. Difference strain energy mode shapes obtained on an aluminum beam. Damage at locations 38 and 47.

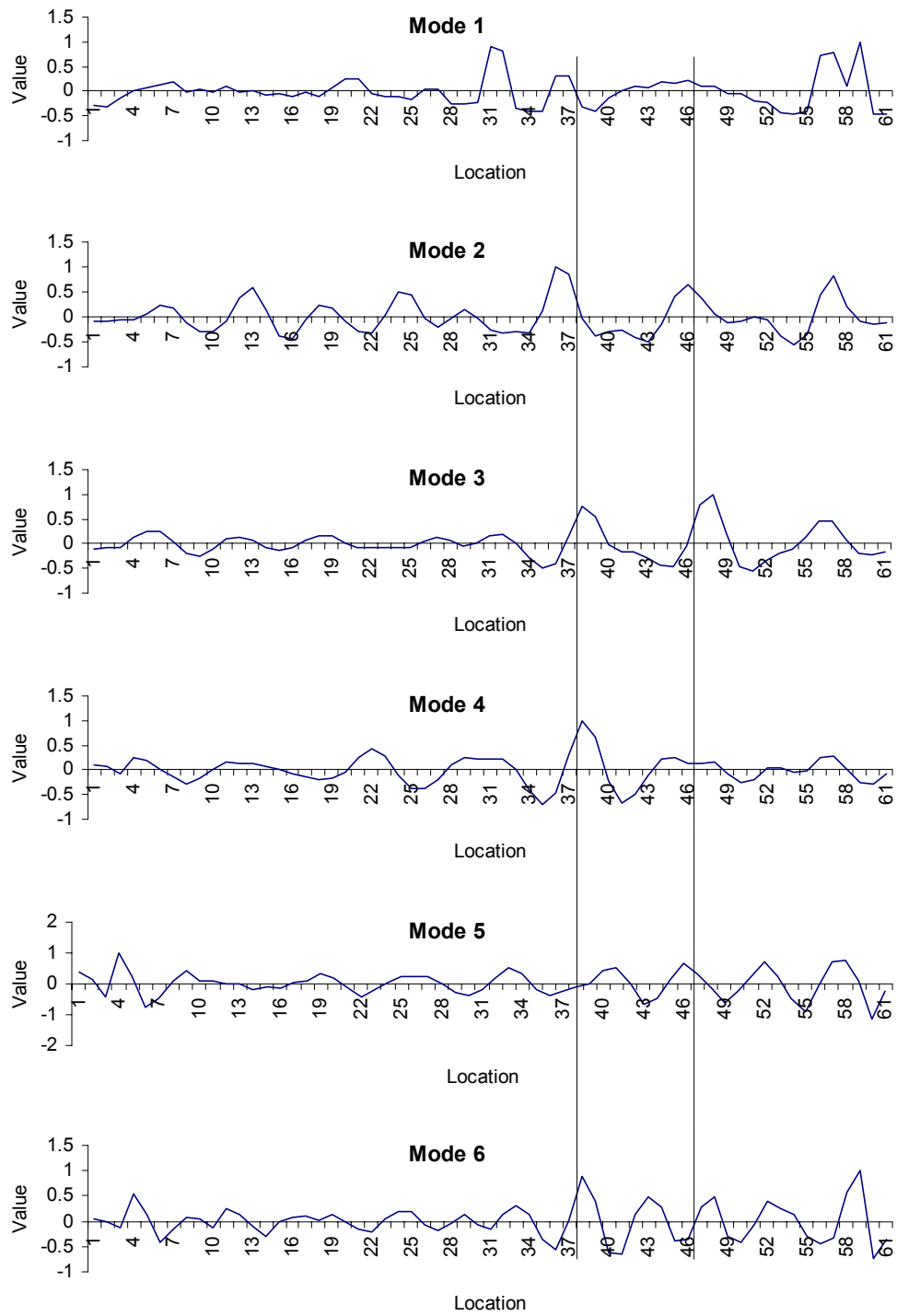


Figure 8. Modified spectrum strain energy mode shapes for an aluminum beam. Damage at locations 38 and 47.

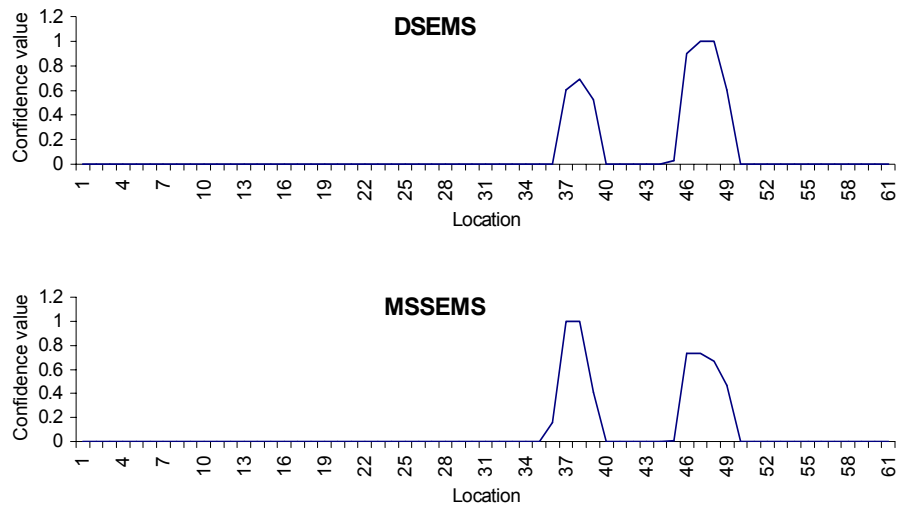


Figure 9. Results of the automated damage detection on the data from Figure 7 and Figure 8.